THE JOURNAL OF BIOLOGICAL CHEMISTRY VOL. 284, NO. 46, pp. 32075–32088, November 13, 2009

Cysteine Residues in the Large Extracellular Loop (EC2) Are Essential for the Function of the Stress-regulated Glycoprotein M6a*

Received for publication, April 24, 2009, and in revised form, August 25, 2009 Published, JBC Papers in Press, September 8, 2009, DOI 10.1074/jbc.M109.012377

Beata Fuchsova[1], **María E. Fernández, Julieta Alfonso, and Alberto C. Frasch**[2]

From the Instituto de Investigaciones Biotecnológicas-INTECH, Universidad Nacional de San Martín, Consejo Nacional de Investigaciones Científicas y Técnicas, 1650 San Martin, Argentina

Gpm6a **was identified as a stress-responsive gene in the hippocampal formation. This gene is down-regulated in the hippocampus of both socially and physically stressed animals, and this effect can be reversed by antidepressant treatment. Previously we showed that the stress-regulated protein M6a is a key modulator for neurite outgrowth and filopodium/spine formation. In the present work, mutational analysis was used to characterize the action of M6a at the molecular level. We show that four cysteines 162, 174, 192, and 202 within EC2 are functionally crucial sites. The presence of cysteines 162 and 202 is essential for the efficient cell surface expression of the M6a protein. In contrast, cysteines 174 and 192, which form a disulfide bridge as shown by biochemical analysis, are not required for the efficient surface expression of M6a. Their mutation to alanine does not interfere with the localization of M6a to filopodial protrusions in primary hippocampal neurons. The neurons expressing C174A and/or C192A mutants display decreased filopodia number. In non-permeabilized cells, these mutant proteins are not recognized by a function-blocking monoclonal antibody directed to M6a. Moreover, neurons in contact with axons expressing C174A/C192A mutant display significantly lower density of presynaptic clusters over their dendrites. Taken together, this study demonstrates that cysteines in the EC2 domain are critical for the role of M6a in filopodium outgrowth and synaptogenesis.**

Glycoprotein M6a is a neuronally expressed member of the proteolipid protein (PLP/DM20) family (1) whose gene has been identified as a stress-responsive gene in the hippocampal formation. In several animal models of chronic stress, expression levels for M6a in hippocampal tissue were found to be diminished by chronic stress exposure and this effect was counteracted by treatment with antidepressants (2–3). Recently, an association of the *M6A* gene with the subgroup of schizophrenia patients with high levels of depression has been reported (4). These findings suggest that M6a plays a role in the stress-induced hippocampal alterations that are found in psychiatric disorders in general. M6a is prominently expressed in the central nervous system as early as embryonic day 10 and remains detectable in adulthood (5). Originally, it was identified as an antigen reacting with the monoclonal M6 antibody and its role as a modulator of neurite outgrowth was postulated (6). Lagenaur *et al.* (6) demonstrated that IgG or Fab fragments of M6 antibody interfere with the extension of neurites by cultured cerebellar neurons. A recent study by Zhao *et al.* (7) shows that M6a expressed in the murine neural retina also regulates neurite extension. The neurite outgrowth of M6a-overexpressing retinal cells was strikingly enhanced, although M6a did not affect differentiation and proliferation.

Even though the precise biological function of M6a still remains unclear, there is a growing body of evidence indicating the importance of M6a in the processes of neural development such as neurite extension and differentiation. For example, a study by Mukobata *et al.* (8) reported that M6a expression enhances nerve growth factor-primed neurite extension in rat pheochromocytoma PC12 cells. They show that it also induces an increase in the intracellular Ca^{2+} concentration of PC12 cells and that the anti-M6a antibody efficiently interferes with both nerve growth factor-triggered Ca^{2+} influx and neurite extension (8). Next, inhibition of mouse M6a expression was found to lead to decreased differentiation of neurons derived from mouse embryonic stem cells (9). Furthermore, it has been demonstrated that M6a plays an important role in neurite/filopodium outgrowth and synapse formation (10). This study shows that M6a overexpression induces neurite formation and increases filopodia density in hippocampal neurons. *M6a* knockdown with small interference RNA methodology showed that M6a low expressing neurons display decreased filopodia number and a lower density of synaptophysin clusters. The reduced M6a expression by chronic stress might be directly related to the morphological alterations found in the hippocampus of chronically stressed animals. The mechanism that would explain how M6a regulates neurite/filopodium outgrowth and its involvement in chronic stress response remains unclear.

In this study our goal was to identify the regions within M6a that are critical for the neurite/filopodium outgrowth. To define the putative biologically critical amino acid residues we took advantage of the striking structural similarities that M6a bears to the tetraspanin family of proteins. The functional spec-

* This work was supported in part by an international Research Scholars grant from the Howard Hughes Medical Institute (to A. C. F.) and the Agencia Nacional de Promocion Cientifica y Tecnologica.

[1] To whom correspondence should be addressed: Instituto de Investigaciones Biotecnologicas, Universidad Nacional de San Martin, Edificio 24, INTI, Av. General Paz 5445, 1650 San Martin, Buenos Aires, Argentina. Tel.: 54-11-4580-7255; Fax: 54-11-4752-9639; E-mail: beata@iib.unsam.edu.ar.

[2] Researcher from the National Council for Research (CONICET).

ificity of tetraspanins is determined by the EC2[3] region. The EC2 is subdivided into a constant region and a variable region. The variable subdomain, which contains nearly all of the known tetraspanin protein-protein interaction sites, is inserted within the conserved subdomain and their relative topology is governed by the occurrence of key disulfides. The central role of the two disulfide bridges in stabilizing the EC2 structure was firmly established. In addition, most EC2s of tetraspanins are glycosylated in one or more potential *N*-glycosylation sites (11–14).

Similarly to tetraspanins, the extracellular region of M6a contains cysteines residues that may be functionally crucial sites. In this report, we show that cysteines 174 and 192 within the EC2 are important for the role of the M6a protein in filopodia formation and synaptogenesis.

EXPERIMENTAL PROCEDURES

Site-directed Mutagenesis—All mutations were introduced into GFP-M6a, a mammalian expression plasmid coding for wild type (WT) M6a fused with green fluorescent protein (GFP) that has been described previously (10). The expressed fusion protein is functional and localizes correctly to the plasma membrane of transfected cell lines or neuronal primary cultures. To create the cysteine mutants, cysteine residues at positions 44, 46, 162, 174, 192, and 202 were mutated to alanine. The substitution of conserved cysteine residues with alanine rather than serine has been proposed to minimize the effects of the substituting amino acid on proper protein folding and stability (15). To mutate two *N*-glycosylation sites, asparagines at positions 164 and 208 were substituted by glutamines. Multiple mutations in EC2, where two or more cysteines (Cys^{162}, Cys^{174}, Cys^{192}, and Cys^{202}) or two asparagines (Asn^{164} and Asn^{208}) were mutated, were created by conducting serial rounds of site-directed mutagenesis. The desired mutations were generated by standard PCR mutagenesis techniques using BD Advantage 2 Polymerase Mix (BD Biosciences Clontech). Two overlapping oligonucleotide primers, one of which contains the target mutation (purchased from Sigma) were used to amplify the template DNA and were as follows: C44A forward, 5′-T GGC TGT GGC CAT GAA GCC CTT TCT GGA ACA-3′, reverse, 5′-AAG GGC TTC ATG GCC ACA GCC AGC GAA CAG GGC AA-3′; C46A forward, 5′-T GGC CAT GAA GCC CTT TCT GGA ACA GTC AA-3′, reverse, 5′-AGA AAG GGC TTC ATG GCC AGC GCC ACA GAA CA-3′; double C44A/C46A forward, 5′-T GGC CAT GAA GCC CTT TCT GGA ACA GT-3′, reverse, 5′-A AAG GGC TTC ATG GCC AGC GCC AGC GAA CAG GGC AA-3′; C162A forward, 5′-TC AAT GTG TGG ACC ATC GCC CGG AAC ACC A-3′, reverse, 5′-GAT GGT CCA CAC ATT GAA ATA CAT GTA CAC GGG C-3′; C174A forward, 5′-TA GTG GAG GGA GCA AAT CTC GCC TTG GAT CTG-3′, reverse, 5′-GAG ATT TGC TCC CTC CAC TAG AGT GGT GTT-3′; C192A forward, 5′-CA ATT GGA GAG GAA AAG AAA ATT GCT ACT GCC TCT G-3′, reverse, 5′-AAT TTT CTT TTC CTC TCC AAT TGT CAC AAT CCC-3′; C202A forward, 5′-CT GAG AAC TTC CTG AGG ATG GCT GAA TCT ACT-3′, reverse, 5′-CAT CCT CAG GAA GTT CTC AGA GGC AGT ACA-3′; N164Q forward, 5′-C AAT GTG TGG ACC ATC TGC CGG CAA ACC ACT C-3′, reverse, 5′-CCG GCA GAT GGT CCA CAC ATT GAA ATA CAT GTA CAC G-3′; N208Q forward, 5′-G AGG ATG TGT GAA TCT ACT GAG CTG CAG ATG ACC TTC CAC-3′, reverse, 5′-CAG CTC AGT AGA TTC ACA CAT CCT CAG GAA GTT CTC AGA GGC-3′. Following temperature cycling, the DpnI endonuclease was used to digest the parental DNA template and to select for mutation-containing synthesized DNA. The identity of all mutant constructs were verified by DNA sequencing on ABI 377 or ABI 3130 sequencers (Applied Biosystems).

Hippocampal Cultures, Cell Lines, and Plasmid Transfections—Dissociated neuronal cultures were prepared from hippocampi of embryonic day 19 Wistar rats, as described (16). Briefly, tissue was treated with 0.25% trypsin in Hanks' solution for 15 min at 37 °C. A single-cell solution was prepared in Eagle's minimal essential medium (MEM) containing 2 mM glutamine, 10 μM sodium pyruvate, 100 units/ml penicillin, and 100 μg/ml streptomycin (MEM1X) with 10% (v/v) horse serum. Cells were seeded on plates or coverslips coated with 0.1 mg/ml poly-L-lysine hydrobromide (Sigma) and 20 μg/μl laminin (Invitrogen) at a density of 20,000 cells/cm^2. After 2 h, medium was changed to MEM/N2 (MEM1X with 1 g/liter ovalbumin and B27 serum-free supplements from Invitrogen). Mouse neuroblastoma N2a and COS-7 cells were cultured in Dulbecco's modified Eagle's medium with 10% (v/v) fetal bovine serum, penicillin, and streptomycin. Neurons or N2a cells growing in 24-well plates were transiently transfected with 2 μg of DNA mixed with 1 and 2 μl of Lipofectamine 2000 (Invitrogen), respectively, following the manufacturer's instructions (medium was changed 4–6 h later).

Immunocytochemistry—Cells were fixed in 4% paraformaldehyde, 4% sucrose in phosphate-buffered saline (PBS) for 20 min at room temperature. If not indicated otherwise in the text, fixation was followed by permeabilization with 0.1% Triton X-100 in PBS for 2 min. Cultures were blocked with 3% bovine serum albumin in PBS for 1–2 h followed by incubation with the primary antibody in 3% bovine serum albumin at 4 °C overnight and with secondary antibodies at room temperature for 1 h. Primary antibodies were: monoclonal anti-M6a rat IgG (1/250) (Medical and Biological Laboratories), monoclonal anti-microtubule-associated protein 2 (MAP2) mouse IgG (1/200) (Sigma), and anti-synaptophysin 1 rabbit antiserum (1/500) (Synaptic Systems, Gottingen, Germany). Secondary antibodies were goat anti-rabbit IgG conjugated to Alexa Fluor 568 (1/1000), goat anti-mouse IgG conjugated to Alexa Fluor 350 (1/200) (Molecular Probes), or rhodamine red-conjugated goat anti-rat IgG (1/1000) (Jackson). F-actin was stained with rhodamine phalloidin (1/1000) (Molecular Probes), together with secondary antibody incubation in the case of double labeling experiments. Coverslips were mounted in FluorSave Reagent (Calbiochem). Fluorescent images were acquired by using

[3] The abbreviations used are: EC2, large extracellular loop; EC1, small extracellular loop; PLP, proteolipid protein; WT, wild type; GFP, green fluorescent protein; N2a, mouse neuro-2a neuroblastoma cell line; PBS, phosphate-buffered saline; MAP2, microtubule-associated protein 2; PK, proteinase K; mAb, monoclonal antibody; TMD, transmembrane domain; MEM, minimal essential medium; ANOVA, analysis of variance; MTSEA, *N*-biotinylaminoethyl methanethiosulfonate.

a Nikon E600 microscope equipped with epifluorescence illumination (Nikon) with a ×100 oil-immersion lens.

Proteinase K Treatment and Western Blotting—COS-7 cells in 100-mm plates were grown to 90% confluence and transfected with plasmids encoding WT GFP-M6a fusion protein or double C174A/C192A mutant protein (24 μg of DNA) using Lipofectamine 2000 (Invitrogen) following the manufacturer's instructions. Twenty-four hours following the transfection, cells were rinsed with PBS and incubated with PBS alone or with proteinase K (PK) at a final concentration 1 mg/ml (Promega) for 30 min at 37 °C. At the end of the incubation, dishes were placed on ice and 0.5 mM phenylmethylsulfonyl fluoride was added to halt digestion. Cells were scraped and transferred to Eppendorf tubes. Samples were then rapidly centrifuged, and the supernatants were aspirated. Cell pellets were lysed in a modified RIPA buffer (150 mM NaCl, 50 mM Tris-HCl, 1% deoxycholate sodium salt, 0.1% SDS, pH 8) supplemented with protease inhibitor mixture (Sigma) for 15 min on ice. Proteins were then precipitated by trichloroacetic acid/acetone precipitation at −20°C overnight. After the precipitation, samples were centrifuged at 11,500 × *g* for 15 min at 4°C, and the supernatants were discarded. The protein pellets were dissolved in the appropriate volume of rehydration buffer (10 mM dithiothreitol, 20 mM Tris-HCl, pH 6.8, 9 M urea) and the concentration of solubilized proteins measured using a Bradford assay (Bio-Rad Protein Assay). 5× SDS sample buffer was added to each sample. The protein samples were loaded on 10% SDS-polyacrylamide gels (15 μg/lane) and transferred to a nitrocellulose membrane by electroblotting. After 2 h of blocking in Tris-buffered saline containing 5% nonfat dried milk, the membranes were incubated with rabbit anti-GFP polyclonal serum (1/750) (Invitrogen). Antigen-antibody complexes were detected using an anti-rabbit horseradish peroxidase-linked secondary antibody (1/10,000) (Dako, Denmark) according to standard Enhanced Chemiluminescence (ECL) Western blotting protocol using Super Signal West Pico chemiluminescent substrate (Pierce).

Cell Surface Biotinylation of Free Cysteines—Cell surface protein were biotinylated with *N*-biotinylaminoethyl methanethiosulfonate (MTSEA-biotin; Toronto Research Chemicals). MTSEA-biotin is a membrane-impermeable, thiol-reactive agent that reacts only with cysteinyl sulfhydryl groups of free cysteines. Thus only cysteines not in a disulfide bond and in an accessible area of the protein tertiary structure will form a mixed disulfide with this alkylthiosulfonate and can be detected on immunoblots of avidin-biotin pulldown assays. No biotinylation would indicate that all cysteines in the extracellular region are unavailable, either from being disulfide-bonded and/or from residing in an area of the molecule that is inaccessible to MTSEA-biotin. A Cys → Ala point mutation of a residue that normally forms a disulfide bond would result in the bond being broken and the liberation of a partner cysteine residue would be detected as an increase in the biotinylation. In case of a double Cys → Ala mutation, when the correct pair of cysteines in a disulfide bond had been mutated the MTSEA-biotinylation would be decreased. In contrast, a double mutation corresponding to incorrect partners may result in an increase in biotinylation because of formation of a further free cysteine residue. COS-7 cells in 100-mm plates were grown to 90% confluence and transfected with plasmids encoding GFP-tagged WT M6a, PLP, and the indicated M6a mutants (20 μg of DNA) using Lipofectamine 2000 (Invitrogen) following the manufacturer's instructions. Twenty-four hours following transfection, cells were rinsed twice with ice-cold PBS and incubated with MTSEA-biotin (at a final concentration 0.5 mM) in PBS for 30 min at 4 °C. Unbound MTSEA-biotin in the reaction was quenched by 50 mM NH_4Cl. Cells were washed twice in 25 mM Tris, 150 mM NaCl, pH 7.2, scraped, and transferred to Eppendorf tubes with 500 μl of lysis buffer (10 mM Tris, 150 mM NaCl, 5 mM EDTA, 1% Triton X-100, pH 7.2) supplemented with a protease inhibitor mixture (Sigma). Cells were disrupted by sonicating on ice using five 1-s bursts and incubated on ice for 30 min. After centrifugation at 10,000 × g for 2 min at 4°C, 400 μl of the clarified supernatant was added to 400 μl of NeutrAvidin-agarose slurry (Pierce) pre-equilibrated according to the manufacturer's instructions. Samples were rotated overnight at 4 °C to allow binding of neutravidin to biotinylated proteins. Then, the beads were washed three times with washing buffer (10 mM Tris, 150 mM NaCl, 5 mM EDTA, 1% Triton X-100, 1% deoxycholate, pH 7.2) with a 2-min centrifugation (1,000 × *g*) at 4 °C between washes. After the final wash, biotinylated proteins were eluted by 2 × 50 μl of 1× SDS sample buffer with 100 mM dithiothreitol and boiled for 5 min before SDS-PAGE and Western blotting analyses. The remaining 100 μl of clarified cell lysate was used to assess the total amount of the overexpressed GFP-tagged protein in cellular lysate (input control for quantification purposes). Proteins were precipitated by trichloroacetic acid/acetone precipitation as described above, dissolved in 20 μl of rehydration buffer, and the concentration of solubilized proteins was measured using the Bradford assay (Bio-Rad protein assay). 5× SDS sample buffer was added to each sample. The protein samples were loaded on 10% SDS-polyacrylamide gels, transferred to a nitrocellulose membrane by electroblotting, and processed for anti-GFP antibody (rabbit anti-GFP polyclonal serum (1/750); Invitrogen) staining as described previously. Immunoblots were quantified by densitometric analyses using ImageJ software.

Quantification and Statistical Data Analysis—For the neuroblastona cell line N2a, the percentage of cells showing filopodial protrusions (visualized by the F-actin marker phalloidin) was calculated for both transfected as well as non-transfected cells from the same coverslip. Transfection with WT M6a and GFP alone was used as a control. On average, 60–120 cells from three to nine groups for each transfection condition from multiple experiments were analyzed. The ratio of transfected to non-transfected filopodia-bearing cells from the same coverslip was determined. Filopodium density (number of protrusions per 20-μm neurite length measured within 50 μm from the soma as shown in the Fig. 7*A*) was quantified in 33–55 neurites of different neurons from 2 to 12 groups for each overexpression culture from multiple experiments. Group means were then analyzed for overall statistical significance by using one-way ANOVA followed by Dunnett's multiple comparison test for post hoc effects *versus* WT M6a and GFP as controls or by a Student's *t* test. To quantify the spots of synaptohysin 1 immunoreactivity, regions where transfected axons (identified by

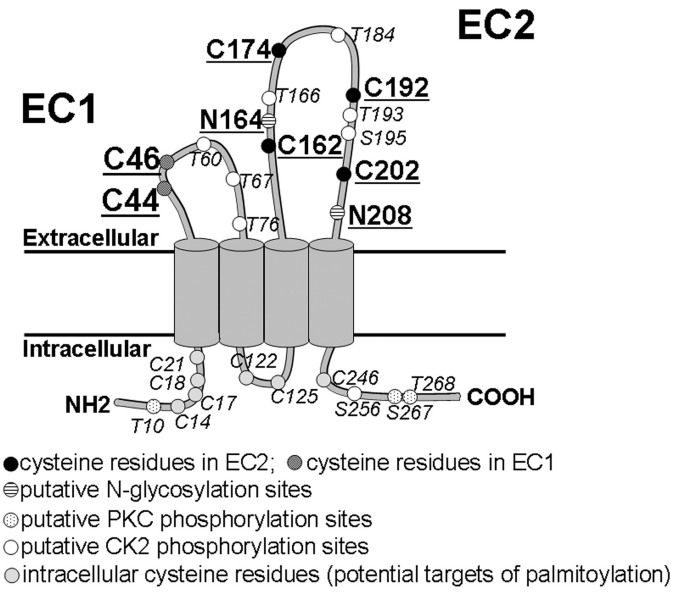

FIGURE 1. **M6a structural features.** The transmembrane topology of the rat M6a based on the secondary structure prediction of membrane proteins from a protein sequence using the SOSUI system. Based on the predicted computational model it contains four transmembrane domains, a small extracellular loop (*EC1*), a very short intracellular loop, and a large extracellular loop (*EC2*), flanked by relatively short N- and C-terminal cytoplasmic tails. The proposed sites of mutation in the extracellular loops are highlighted (cysteine residues in *EC2 C162*, *C174*, *C192*, *C202*, cysteine residues in *EC1 C44*, *C46*, and potential *N*-glycosylation sites *N164*, *N208*).

green labeling and their lack of MAP2 immunostaining) contacted non-transfected MAP2 positive dendrites were selected. The number of immunopositive synaptophysin 1 puncta was counted in a 40-μm neurite length along similar distances out from the soma in 22 neurites of a minimum 11 different neurons per group for overexpression cultures and repeated on three separate culture preparations. Group means were then analyzed for overall statistical significance by using one-way analysis of variance (ANOVA) followed by Tukey's multiple comparison tests. Calculations were performed with the software GraphPad Prism.

RESULTS

Mutation of Cysteine Residues in EC2 of M6a; Cysteine Residues 162 and 202 Are Critical for the Correct M6a Localization in the Plasma Membrane—To define the part of the M6a molecule or amino acid residues that might be critical for the induction of filopodial protrusion formation, we constructed a series of M6a mutants expected to interfere with the function of the protein. The selection of proposed mutation sites was based on structural similarity of M6a to tetraspanins and numerous mutational analysis data available on the function of this family of proteins. Fig. 1 shows the predicted computational model of M6a displaying M6a structural features. It contains four transmembrane domains, a small extracellular loop (EC1), a very short intracellular loop, and a large extracellular loop (EC2), flanked by relatively short N- and C-terminal cytoplasmic tails. There are four cysteines residues in EC2 domain (Cys^{162}, Cys^{174}, Cys^{192}, and Cys^{202}) that may be functionally important and two cysteines residues in the EC1 domain (Cys^{44} and Cys^{46}). The EC2 domain also contains two potential *N*-glycosylation sites (Asn^{164} and Asn^{208}). In the cytoplasmic part of the protein, two potential sites for protein kinase C and one for the casein kinase II phosphorylation are present as well as additional juxtamembrane cysteine residues.

In analogy to tetraspanins, function of M6a may be determined by its EC2 region and its four cysteines residues may play the central role. To test this hypothesis, single C162A, C174A, C192A, and C202A point mutations, as well as double C162A/C174A, C174A/C192A, triple C162A/C174A/C192A, and quadruple C162A/C174A/C192A/C202A point mutations were introduced into GFP-M6a.

The constructs were transfected into the neuroblastoma cell line N2a, and subcellular distribution of WT and mutant M6a proteins was analyzed by immunofluorescence microscopy. Fig. 2*A* shows non-permeabilized N2a cells transfected with the WT M6a and mutants. Single C162A and 202A mutants and all variants that include these mutations were detected intracellulary and none of them displays cell surface expression that can be clearly seen in control WT M6a-transfected cells (Fig. 2*A*, *maximized views*). Taken together, these results show that Cys → Ala mutations of Cys^{162} and Cys^{202} in the EC2 region disrupt the cell membrane localization of the M6a protein. We suppose that they could interfere with proper protein folding and/or cell surface trafficking.

On the other hand, when N2a cells were transfected with single C174A or C192A or their combination C174A/C192A M6a mutants, we observed intense staining of the plasma membrane (Fig. 2*A*). To determine whether the C174A/C192A mutant was exposed on the outside of the cell, we probed its accessibility to digestion with the extracellular PK, a broad spectrum protease widely used to demonstrate the surface exposure of the membrane proteins. If WT M6a or the C174A/C192A mutant were expressed on the plasma membrane, their extracellular part would be accessible to PK digestion. Intracellular parts of the proteins would be inaccessible, and thus protected from PK digestion. On Western blot we would be able to detect the fragments undigested by PK. Using anti-GFP antibody we expected to detect a cleaved fragment (~32 kDa) corresponding to the GFP-tagged N-terminal part including the first transmembrane domain after PK treatment. In case the proteins are not cell surface exposed, and thus inaccessible to protease digestion, only full-length GFP fusion proteins would be detected by anti-GFP antibody after PK treatment. Intact COS-7 cells transfected with the double C174A/C192A mutant or WT M6a as a control were treated with PK. Cleaved products were analyzed on immunoblots using anti-GFP antibody. In both cases, PK treatment of cells expressing either WT M6a or the double C174A/C192A mutant yielded protein fragments of ~32 kDa (Fig. 2*B*), which is consistent with the size of the N-terminal GFP-tagged fragment localized inside the cell. This indicates that the mutant protein is accessible to PK digestion, and thus present on the plasma membrane.

Detection of Disulfide Bonds in the Extracellular Region of M6a—To investigate whether cysteine residues within the extracellular region of M6a form disulfide bonds, MTSEA-biotin labeling of cell surface proteins was performed. We used this assay to assess the availability of accessible free cysteines in the extracellular region of WT M6a and M6a cysteine mutants.

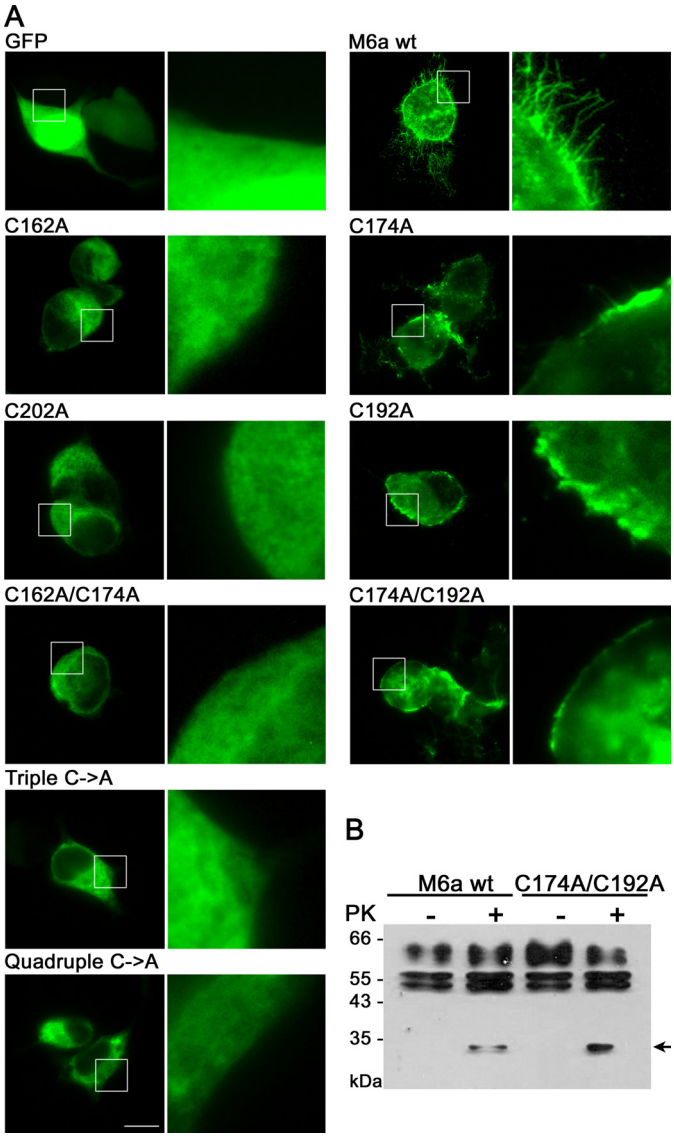

FIGURE 2. *A*, subcellular distribution of EC2 cysteine M6a mutants. Images show the intracellular distribution of the C162A, C202A, double C162A/C174A, triple Cys → Ala, and quadruple Cys → Ala mutants and the membrane localization of the M6a WT, C174A, C192A, and double C174A/C192A mutants in the neuroblastoma N2a cell line. N2a cells were transfected with the indicated GFP-tagged mutants, and WT GFP-M6a and GFP alone as controls. Fluorescent images were acquired with a ×100 oil-immersion lens. Mutations of Cys^{162} and Cys^{202} in the EC2 region prevent surface expression of the M6a mutants. Mutation of Cys^{174} and Cys^{192} in the EC2 region allows surface expression of M6a mutants. *Bar* = 10 μm. *B*, both M6a WT and C174A/C192A are accessible to digestion with proteinase K. Intact COS-7 cells transfected with WT M6a and C174A/C192A mutant M6a were treated with PK (1 mg/ml) for 30 min at 37 °C. Immunoblot analysis of cell lysates before (−) and after (+) PK treatment shows undigested fragments of ~32 kDa (*arrow*) resulting from proteolytic cleavage of cell surface-exposed proteins after (+) PK treatment.

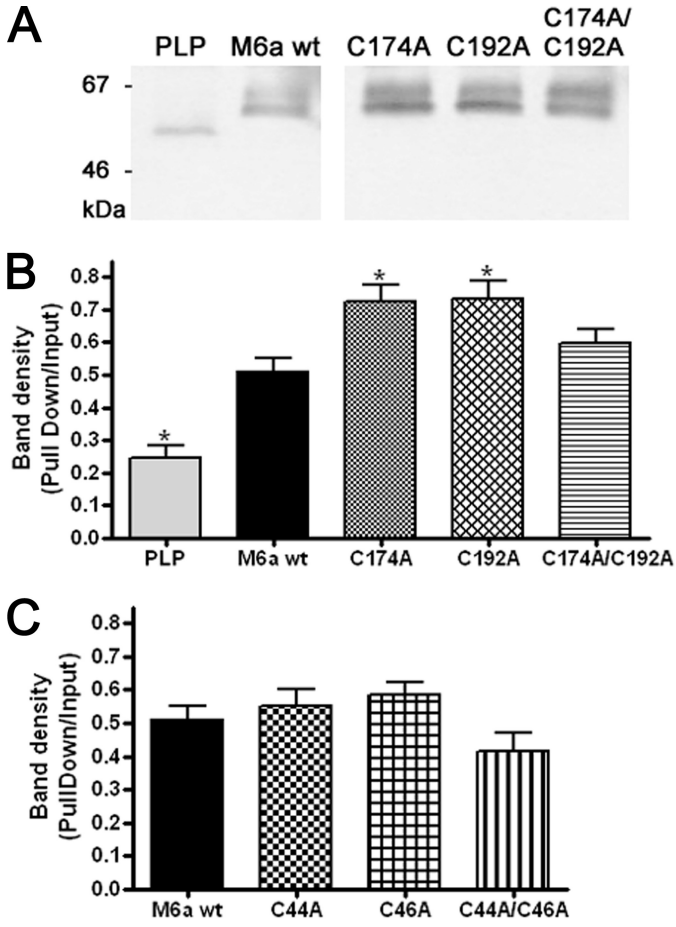

FIGURE 3. **Detection of free cysteine residues in WT M6a and cysteine mutants of M6a using MTSEA-biotin labeling.** *A*, anti-GFP antibody probed immunoblot of cell surface-biotinylated proteins pulled down by neutravidin from supernatants of WT GFP-M6a, and the indicated GFP-tagged M6a mutant-transfected COS-7 cells previously incubated in MTSEA-biotin. Transfection with WT GFP-PLP was used as a control. *B* and *C*, densitometric analysis of immunoblots. Data are shown as the ratio of biotinylated proteins pulled down by neutravidin to the total in cellular lysates. By SDS-PAGE, M6a migrates as multiple bands due to posttranslational modifications of the protein (such as phosphorylation and glycosylation). Density of the broad band was measured for quantification purposes. *B*, biotinylation of EC2 cysteine mutants of M6a. A significant increase in biotinylation was detected for C174A and C192A when compared with WT M6a. The biotinylation of the double C174A/C192A mutant does not differ from that of WT M6. One-way ANOVA, ***, p value <0.0001; Dunnett's multiple comparison test, *, $p < 0.01$ M6a WT *versus* PLP; *, $p < 0.01$ M6a WT *versus* C174A; *, $p < 0.01$ M6a WT *versus* C192A; $p > 0.05$ M6a WT *versus* C174A/C192A. *C*, biotinylation of EC1 cysteine mutants of M6a. The biotinylation of C44A and C46A does not differ from that of WT M6a. The double C44A/C46A mutant showed a decrease in biotinylation compared with WT M6a although the difference was not statistically significant. One-way ANOVA, p value 0.1003; Dunnett's multiple comparison test, $p > 0.05$ M6a WT *versus* C44A; $p > 0.05$ M6a WT *versus* C46A; $p > 0.05$ M6a WT *versus* C44A/C46A. Data plotted represent means ± S.E. Data are representative of two independent experiments.

Intact COS-7 cells transfected with GFP-tagged WT M6a, and the indicated M6a cysteine mutants, were treated with MTSEA-biotin. GFP-tagged PLP was used as a control because it belongs to the same family of proteins as M6a and the state of all cysteines residues of PLP and its membrane topology are well known (17). Cell surface-biotinylated proteins were pulled down by neutravidin and analyzed on immunoblots using anti-GFP antibody. For quantification purposes we show data as the ratio of biotinylated proteins pulled down by neutravidin to the total in cellular lysates, as measured by densitometric analysis of immunoblots. Fig. 3, *A* and *B*, demonstrates that WT M6a as well as PLP are biotinylated, indicating that some cysteines in the extracellular region of WT molecules are free and thus accessible to MTSEA-biotin. A further increase in the biotinylation was detected for C174A and C192A mutants. This indicates that these residues are normally involved in disulfide bond formation in WT M6a. Double C174A/C192A mutant showed a decrease in biotinylation, and thus, less free cysteines available for MTSEA-biotinylation (Fig. 3, *A* and *B*).

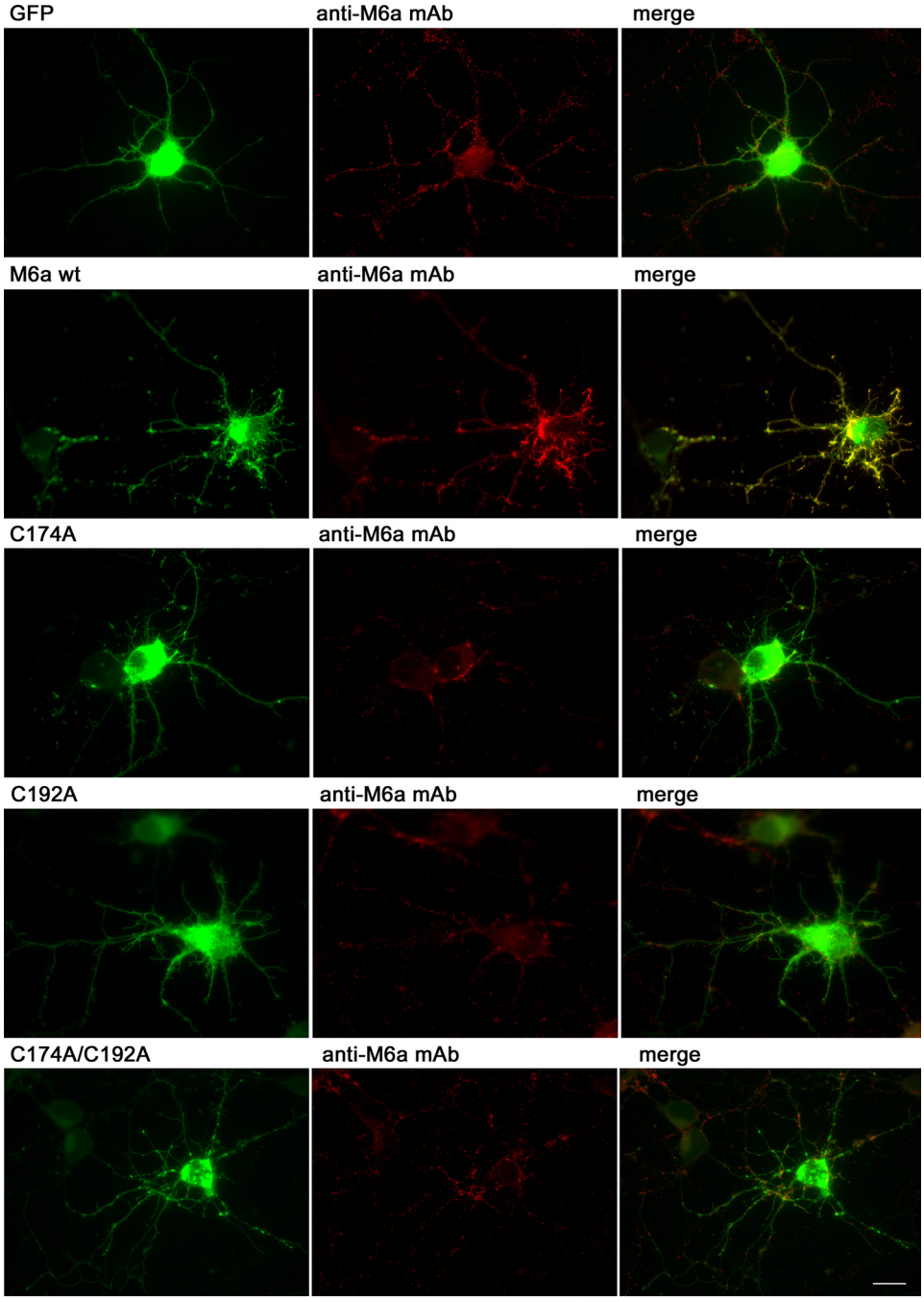

FIGURE 4. **Mutations of Cys^{174} and Cys^{192} in EC2 region prevent epitope recognition by anti-M6a mAb.** Images show complete colocalization in control cells (M6a WT) but no overlap in cells transfected with mutants (the red signal represents endogenous M6a). Primary hippocampal neurons were transfected with the indicated GFP-tagged mutants and fixed as described under "Experimental Procedures." Immunostaining was done with rat anti-M6a mAb in non-permeabilized cells. Goat anti-rat IgG labeled with Alexa Fluor 546 was used as a secondary antibody. Wild type GFP-tagged M6a was used as a control. *Bar* = 10 μm.

This suggests that Cys^{174} and Cys^{192} correspond to the disulfide pair in WT M6a. Biotinylation of C44A and C46A mutants did not differ from that of WT M6a. The double C44A/C46A mutant showed a decrease in biotinylation compared with WT M6a, although the difference was not statistically significant (Fig. 3*C*). It was not possible to test for the cell surface MTSEA-biotinylation of Cys^{162} and Cys^{202} because their mutation to alanine interfered with cell surface expression of the mutant proteins.

Mutation of Cysteines 174 and 192 Prevents Epitope Recognition by a Function Blocking Anti-M6a mAb—The model for M6a topography predicts that EC2 is positioned on the outside of the cell. A previous study reported that monoclonal anti-M6a antibody directed against the extracellular part of the protein interferes with the extension of neurites by cultured cerebellar neurons (6). Interestingly, mutagenesis studies of tetraspanins demonstrated that EC2 of tetraspanins is a crucial site for specific functional protein-protein interactions (18, 19). It contains nearly all of the known tetraspanin protein-protein interaction sites and, in addition, monoclonal antibodies that recognize cell surface epitopes so far exclusively recognize EC2 (19–21).

Thus, we were interested whether the Cys^{174} and Cys^{192} mutations in EC2 of M6a would interfere with binding of the anti-M6a antibody that recognizes a surface-exposed epitope and has been reported to affect neurite extension (6). Primary hippocampal neurons, as well as N2a cells, were transfected with the indicated GFP-tagged mutants. Immunostaining was performed in non-permeabilized cells with rat anti-M6a mAb. Wild type GFP-tagged M6a was used as a control. We show that the surface-exposed region of WT GFP-tagged M6a is recognized by anti-M6a antibody in hippocampal neurons (Fig. 4). The complete colocalization can be observed in the merge image. In contrast, the cells transfected with C174A, C192A, and double C174A/C192A mutants do not display any overlap in the merge image. The same results were observed when neuroblastoma N2a cells were transfected (data not shown). We conclude that although C174A and/or C192A express on the plasma membrane (Fig. 2, *A* and *B*), they do not bind to the function blocking anti-M6a antibody.

Mutation of Cysteine Residues in EC1 Does Not Affect the Cell Membrane Localization of M6a Protein or Its Recognition by a Function Blocking Anti-M6a mAb—As shown Fig. 1, the extracellular region of M6a contains apart from the EC2 domain also a small extracellular loop (EC1) that could potentially be

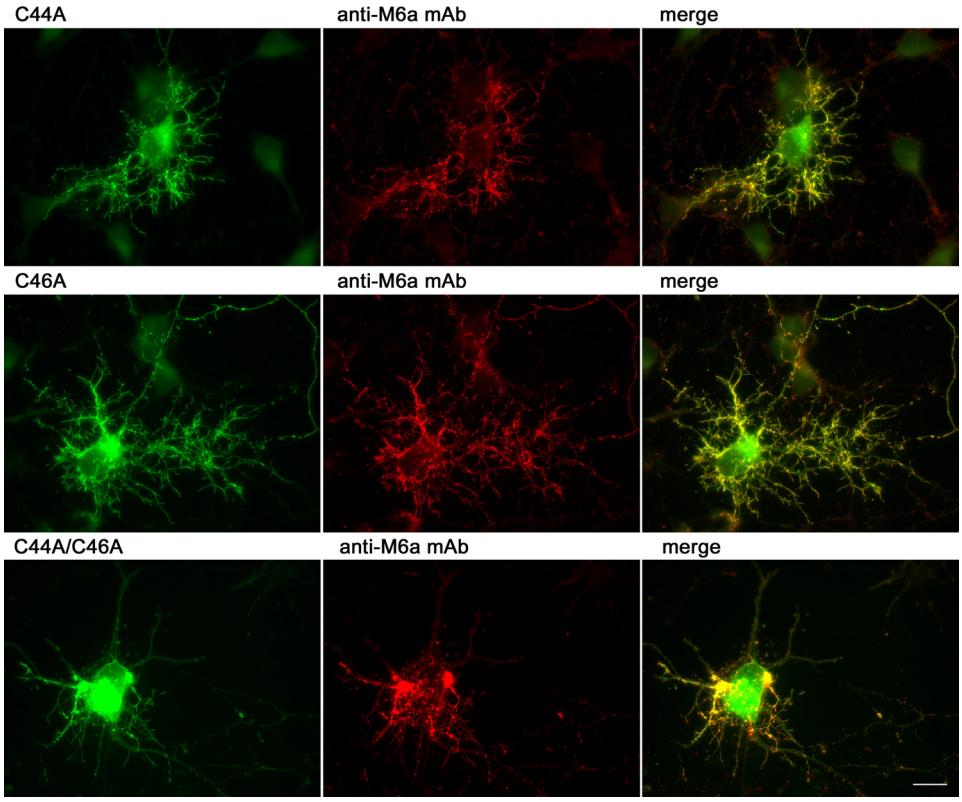

FIGURE 5. **Mutations of Cys^{44} and Cys^{46} in the EC1 region do not prevent epitope recognition by mAb against M6a.** Primary hippocampal neurons were transfected with the indicated GFP-tagged mutants and fixed as described under "Experimental Procedures." Immunostaining was done with rat anti-M6a mAb in non-permeabilized cells. Goat anti-rat IgG labeled with Alexa Fluor 546 was used as a secondary antibody. Images show complete colocalization in cells transfected with mutants C44A, C46A, and C44A/C46A. *Bar* = 10 μm.

involved in anti-M6a antibody binding and/or play a role in the induction of filopodial protrusion formation. There are two cysteines residues (Cys^{44} and Cys^{46}) in the EC1 domain of M6a that attracted our attention as suitable candidates for mutational analysis. Single C44A and C46A point mutations, as well as the double C44A/C46A point mutation were introduced into GFP-M6a. When N2a cells were transfected with these M6a mutants intense staining of the plasma membrane was observed in all three cases (data not shown). Thus, the single C44A, C46A, and double C44A/C46A mutant proteins are able to localize to the plasma membrane the same way as WT M6a.

To test whether EC1 of M6a is part of the surface-exposed epitope recognized by the function blocking anti-M6a antibody, primary hippocampal neurons were transfected with the indicated GFP-tagged mutants. Immunostaining was performed in non-permeabilized cells with rat anti-M6a mAb. The results indicate that the surface-exposed regions of C44A, C46A, as well as C44A/C46A GFP-tagged M6a mutants are completely recognized by anti-M6a antibody (Fig. 5). The colocalization can be observed in the merge image. We conclude that EC1 is not the surface-exposed epitope recognized anti-M6a antibody. The mutation of cysteines residues Cys^{44} and Cys^{46} in EC1 does not interfere with the binding of anti-M6a antibody.

C174A and C192A Mutants Do Not Induce Filopodium Formation in the Neuronal Cell Line as well as in Primary Hippocampal Neurons—The effect of C174A and C192A mutations on filopodial protrusion formation was analyzed and the results compared with that obtained with the WT GFP-M6a or GFP alone (10). First, N2a cells were transfected with GFP-tagged mutant proteins, WT protein and GFP alone, and stained with the F-actin marker phalloidin to visualize filopodia. In the Fig. 6*A*, an example of a WT GFP-M6a positive cell shows localization of the fusion protein at filopodia labeled with phalloidin (*maximized views labeled 1*). As can be observed, the expression of the exogenous WT M6a promotes filopodium formation in the neuronal cell line. Non-transfected cells do not form filopodia to the same extent as transfected cells (Fig. 6*A*, red cells, *maximized views labeled 2*). Next, the number of cells showing filopodial protrusions was quantified and the results are displayed as a ratio of transfected to non-transfected filopodia-bearing cells from the same coverslip. Fig. 6*B* demonstrates that the number of cells showing filopodial protrusions in cells transfected with C174A, C192A, and double C174A/C192A mutants is significantly lower than in the WT M6a-transfected N2a cells.

To confirm that C174A and C192A mutations of M6a have the same effect in cells that normally express M6a, we next examined the effect of these mutations on filopodium formation in primary hippocampal neurons. Neurons were transfected on day 3 after plating with the indicated M6a mutants (single C174A, C192A, and double C174A/C192A mutant) or with WT M6a and GFP alone as controls. Neurons were stained with the anti-MAP2 antibody to label dendrites and with the F-actin marker phalloidin to visualize filopodia. Filopodium density (number of protrusions per 20-μm of neurite length) as shown in the enlarged pictures (Fig. 7*A*) was quantified. Fig. 7*B* shows that WT M6a-transfected neurons have a significantly higher number of filopodia than neurons transfected with C174A, C192A, and double C174A/C192A mutants. Thus, it can be concluded that even though localization of the C174A, C192A, and double C174A/C192A M6a mutants does not differ from that of WT M6a, their overexpression does not promote filopodium formation in the neuronal cell line N2a as well as in primary hippocampal neurons.

Effect of C44A and C46A Mutants within the EC1 on Filopodium Formation—To analyze if overexpression of EC1 cysteine mutants would result in a similar alternation of filopodium formation, we examined the effect of C44A and C46A mutations on filopodium formation in the neuroblastoma

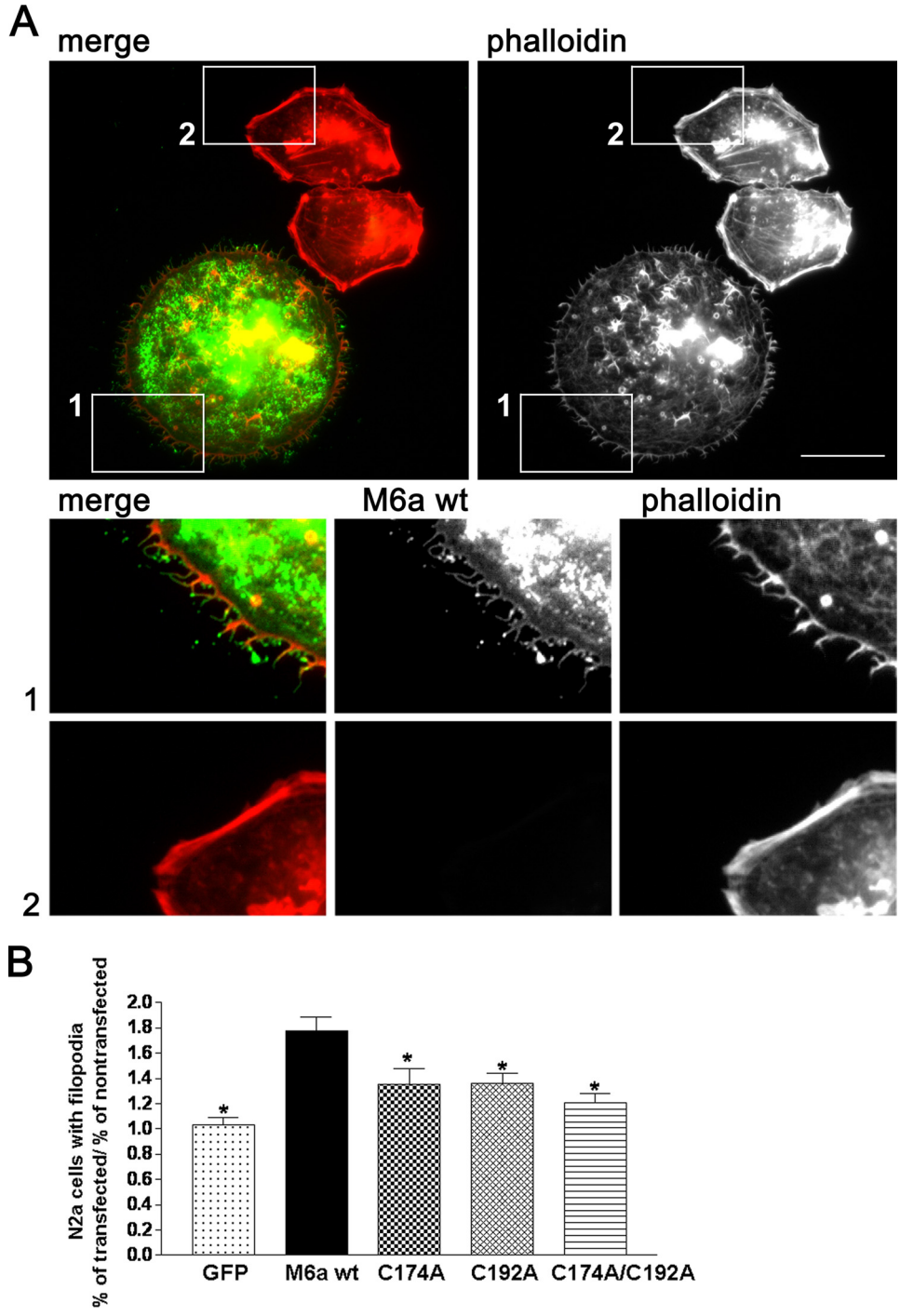

FIGURE 6. **Effect of overexpression of the C174A and C192A mutants on filopodium formation in neuroblastoma.** Overexpression of the C174A, C192A, and double C174A/C192A mutants does not promote filopodium formation in neuronal cells. N2a were transfected with corresponding GFP-tagged mutant proteins, WT protein and GFP alone, fixed and stained with the F-actin marker phalloidin to visualize filopodia. *A*, a WT GFP-M6a positive cell shows localization of the fusion protein at filopodia labeled with phalloidin (*maximized views 1*). Non-transfected N2a cells stained with phalloidin only are also seen (*red* cells, *maximized views 2*). *Bar* = 10 μm. *B*, the number of cells showing filopodium protrusions was quantified and is shown as a ratio of transfected to non-transfected filopodia-bearing cells from the same coverslip. Transfection with WT M6a and GFP alone was used as a control. The number of cells showing filopodium protrusions in cells transfected with C174A, C192A, and double C174A/C192A mutants is significantly lower than in the WT M6a-transfected N2a cells. One-way ANOVA, ***, p value 0.0009; Dunnett's multiple comparison test, *, $p < 0.01$ M6a WT *versus* GFP; *, $p < 0.05$ M6a WT *versus* C174A; *, $p < 0.05$ M6a WT *versus* C192A; *, $p < 0.05$ M6a WT *versus* C174A/C192A. Data are means ± S.E. of ~62–121 cells per group from multiple experiments.

cell line as well as in primary hippocampal neurons. The neuroblastoma cells N2a were transfected with GFP-tagged mutant proteins, WT protein, and GFP alone, and stained with the F-actin marker phalloidin to visualize filopodia. The number of cells showing filopodial protrusions was quantified and the results are displayed as described above. Fig. 8*A* shows that the number of cells showing filopodial protrusions in cells transfected with C44A, C46A, and double C44A/C46A mutants does not significantly differ from that in the WT M6a-transfected N2a cells. Although there is a slight decrease in the number of filopodia formed when cells were transfected with C44A, C46A, or C44A/C46A mutants, the differences with WT M6a were not statistically significant.

Next, we examined the effect of these mutations on filopodial protrusion formation in primary hippocampal neurons. Neurons were transfected on day 3 after plating with the indicated M6a mutants or with WT M6a and GFP alone as controls. Filopodium density was quantified (Fig. 8*B*). The neurons transfected with C44A and C46A mutants do not have a significantly different number of filopodia compared with WT M6a-transfected neurons. But in the case of the double C44A/C46A mutant a significant decrease in filopodia formation was observed.

Thus, although the mutations of the Cys^{44} and Cys^{46} in EC1 do not prevent binding of anti-M6a antibody they do slightly interfere with filopodium formation. We suggest that EC1 contributes to the optimal functioning of the protein in the induction of filopodial protrusion formation.

The N-Glycosylation Mutants of M6a in EC2 Are Not Affected in Their Function—To gain a more detailed insight into the functional importance of EC2 we were further interested in finding out whether the replacement of another conserved amino acid residue within

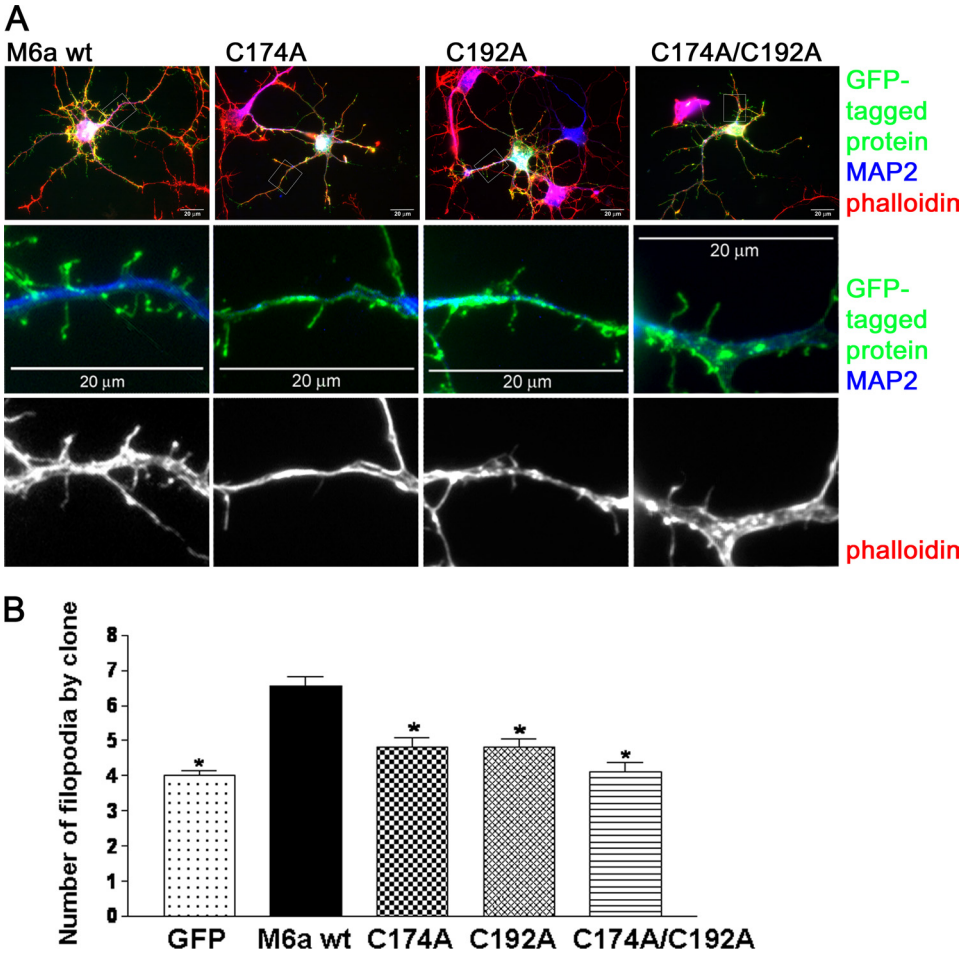

FIGURE 7. **Overexpression of the C174A, C192A, and double C174A/C192A mutants does not promote filopodium formation in primary hippocampal neurons.** *A*, neurons were transfected on day 3 after plating with GFP alone and WT GFP-M6a as controls and with the indicated GFP-tagged M6a mutants (*green*), fixed, and stained with the anti-MAP2 antibody to label dendrites (*blue*), and with the F-actin marker phalloidin to visualize filopodia (*red*). Filopodium density (number of protrusions per 20-μm of neurite length) as shown in the enlarged pictures was quantified. *Bar* = 20 μm. *B*, the graph shows that WT M6a-transfected neurons have a significantly higher number of filopodia than neurons transfected with C174A, C192A, and double C174A/C192A mutants. One-way ANOVA, ***, *p* value 0.0001; Dunnett's multiple comparison test, *, $p < 0.01$, M6a WT *versus* GFP; *, $p < 0.01$, M6a WT *versus* C174A; *, $p < 0.01$, M6a WT *versus* C192A; *, $p < 0.01$, M6a WT *versus* C174A/C192A. Data are means ± S.E. of 38–47 neurites per group from multiple independent experiments.

EC2 different from cysteine would have the same negative effect on filopodium formation or cell membrane localization of the M6a protein. Previous studies have shown that most EC2 tetraspanins are glycosylated in one or more potential *N*-glycosylation sites. Therefore, among the possible sites of interest we focused on the two potential *N*-glycosylation sites that are analogously present in EC2 of M6a (Asn^{164} and Asn^{208}).

To examine the potential involvement of the two *N*-glycosylation sites within the EC2 region in the induction of filopodium formation, asparagines 164 and 208 were substituted by glutamines individually or in combination. When N2a cells were transfected with these M6a mutants intense staining of plasma membrane was observed in all three cases (data not shown). Hence, the Asn → Gln mutations within EC2 did not disrupt the cell membrane localization of M6a protein.

Next, we analyzed the effect of these Asn → Gln mutations on filopodial protrusion formations in neuroblastoma cell lines. The N2a were transfected with GFP-tagged mutant proteins, WT protein, and GFP alone, and stained with the F-actin marker phalloidin. Fig. 9*A* shows that the number of cells showing filopodial protrusions in cells transfected with N164Q, N208Q, and double N164Q/N208Q mutants does not significantly differ from that in the WT M6a-transfected N2a cells. Thus, we conclude that Asn → Gln mutations within the EC2 domain do not interfere with either cell membrane localization of the protein or induction of filopodium formation.

Next, we were interested to see whether the Asn → Gln mutations within EC2 would affect anti-M6a antibody epitope recognition. Primary hippocampal neurons were transfected with the indicated GFP-tagged mutants and fixed as described above. Subsequently, immunostaining was performed in non-permeabilized cells with rat anti-M6a mAb. We show that surface-exposed regions of N164Q, N208Q, as well as double N164Q/N208Q GFP-tagged M6a mutants are completely recognized by anti-M6a antibody in hippocampal neurons (Fig. 9*B*). The complete colocalization can be observed in the merge image. We draw the conclusion that mutation of asparagine residues 164 and 208 within EC2 does not interfere with the binding of the function blocking anti-M6a antibody.

Neurons in Contact with Axons Expressing C174A/C192A Mutant Display Significantly Lower Density of Presynaptic Clusters over Their Dendrites—Synapse formation in the vertebrate central nervous system is a dynamic process, requiring bidirectional communication between pre- and postsynaptic partners. Real time imaging experiments demonstrate that both axonal and dendritic filopodia actively participate in synapse formation (22). In our previous study (10) we have demonstrated that M6a down-regulation using small interfering RNA technology causes not only decreased filopodium density but also reduced synaptic density in hippocampal neurons. Therefore, it seemed interesting to know whether overexpression of the EC2 cysteine C174A/C192A mutant affects synaptic density. It has been shown that synaptic vesicle antigens are concentrated in presynaptic elements at points of contact between axons and appropriate postsynaptic targets in hippocampal cultures (23). To determine the number of synaptic puncta, primary hippocampal neurons after 9 days *in vitro* were transfected with the GFP-tagged C174A/C192A mutant, WT M6a, and GFP alone. Neurons were fixed as described previously and co-im-

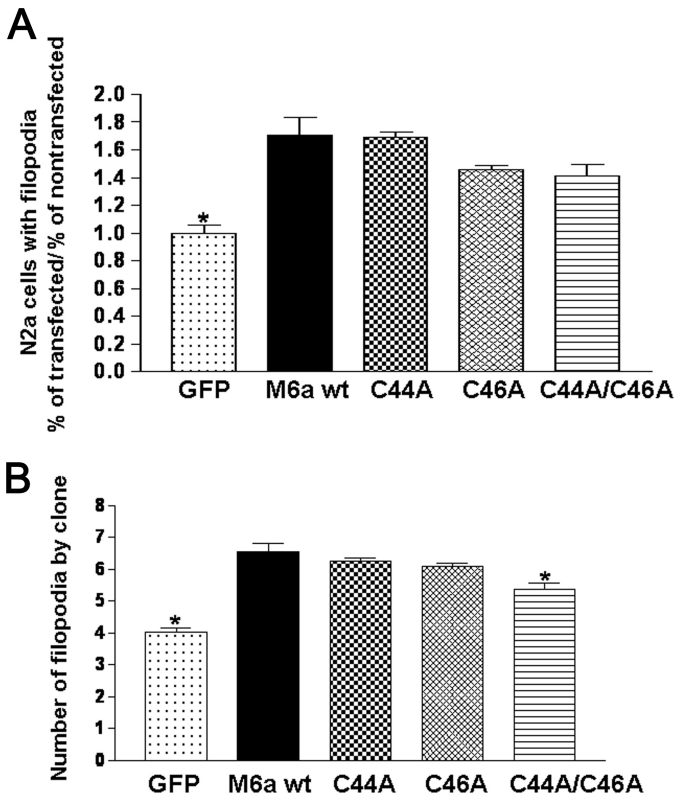

FIGURE 8. **Cysteine residues in the small extracellular domain (EC1).** Effect of the overexpression of C44A, C46A, and double C44A/C46A mutants of M6a on filopodia formation in the neuroblastoma cell line N2a (*A*) and primary hippocampal neurons (*B*). Cells were transfected, fixed, stained, and quantified as described above. *A*, a tendency to a decrease in filopodia formation was observed for M6a mutants C44A, C46A, and C44A/C46A when compared with WT M6a, albeit results were not statistically significant in N2a cells. One-way ANOVA, **, *p* value 0.0022; Dunnett's multiple comparison test, *, $p <$ 0.01, M6a WT *versus* GFP; $p > 0.05$, M6a WT *versus* C44A; $p > 0.05$, M6a WT *versus* C46A; $p > 0.05$, M6a WT *versus* C44A/C46A. Data are means ± S.E. of ~57–133 cells per group from multiple experiments. *B*, a tendency to a decrease in filopodia formation was observed for M6a mutants C44A, C46A, and a significant decrease for C44A/C46A when compared with WT M6a in primary hippocampal neurons. One-way ANOVA, ***, *p* value 0.0001; Dunnett's multiple comparison test, *, $p < 0.01$, M6a WT *versus* GFP; $p > 0.05$, M6a WT *versus* C44A; $p > 0.05$, M6a WT *versus* C46A; *, $p < 0.01$, M6a WT *versus* C44A/C46A. Data are means ± S.E. of 33–55 neurites per group from multiple independent experiments.

munostained with the antibodies against synaptophysin 1 to visualize synaptic puncta and MAP2, a specific marker for dendrites. The number of synaptophysin 1 fluorescent puncta was counted (Fig. 10) in regions where transfected axons (identified by green labeling and their lack of MAP2 immunostaining) contacted non-transfected MAP2 positive dendrites (Fig. 10*A*). Fig. 10*B* shows that dendrites that are in contact with WT M6a expressing axons display significantly higher density of presynaptic clusters compared with the dendrites that are in contact with GFP-transfected axons. On the contrary, overexpression of the C174A/C192A mutant reduces the density of presynaptic clusters over a fixed length of dendrites when compared with WT M6a. Thus, we conclude that Cys^{174} and Cys^{192} mutations within EC2 of M6a not only affects filopodium formation but also synaptic density in hippocampal neurons.

DISCUSSION

The hippocampus is a particularly sensitive and vulnerable brain region that responds to stress and stress hormones. It is known that chronic stress affects the morphology and synaptic organization of the hippocampus, predominantly within CA3 but also CA1 and dentate gyrus (24–29). In our previous studies, we demonstrated that chronic stress induces a decrease in hippocampal mRNA levels for the neuronal membrane glycoprotein M6a shown to modulate neurite outgrowth and filopodium/spine formation (10). The reduced M6a expression by chronic stress has been suggested to be related to the morphological alterations found in the hippocampus of chronically stressed animals. To understand the involvement of M6a in chronic stress response it was imperative to characterize the action of M6a at the molecular level. In the present work, we identify amino acid residues within M6a important for the function of the protein. For the first time, we demonstrate that the second extracellular loop of M6a is critical for the role of the protein in filopodium outgrowth and synaptogenesis. We show the central role played here by four cysteine residues, Cys^{162}, Cys^{174}, Cys^{192}, and Cys^{202}. Among them, Cys^{162} and Cys^{202} are essential for cell surface expression of M6a. Cys^{174} and Cys^{192} are important for the role of M6a in filopodium formation and synaptogenesis. These cysteine residues could play a variety of roles in a protein. Using cell surface MTSEA-biotin labeling of free cysteines we provide here direct biochemical evidence for the existence of the disulfide bond Cys^{174}–Cys^{192} in the EC2 of M6a. The state of Cys^{162} and Cys^{202} could not be directly determined by the MTSEA-biotinylation assay because their mutation to alanine interfered with the cell surface expression of the mutant proteins. Although, the identical phenotypes of C162A and C202A mutants suggests that these residues may form a disulfide bond essential for proper protein folding and/or cell surface trafficking. The biotinylation of WT M6a further indicates also that free cysteines are present in the extracellular region of M6a. No increase in biotinylation of the C44A and C46A mutants compared with WT M6a suggested that these residues are either not involved in disulfide bond formation or their partners in a putative disulfide bond reside in an inaccessible region of the molecule. But because the double C44A/C46A mutant showed a decrease in biotinylation compare to WT M6a we suppose that these two EC1 cysteines are free thiols responsible for biotinylation of WT M6a. Our results completely coincide with the data published on PLP from the same family of proteins, which we used here as a control. In the extracellular region of PLP, four conserved cysteines in EC2 are connected by disulfide bonds: Cys^{200}–Cys^{219} and Cys^{183}–Cys^{227}. On the other hand, Cys^{32} and Cys^{34} are free thiols. We suppose that these two cysteines account for the MTSEA-biotinylation of PLP in our experiment. Because of their localization at the border of the first transmembrane domain (TMD) and EC1 (almost buried in the plasma membrane) they are less accessible to MTSEA-biotin than Cys^{44} and Cys^{46} of M6a, thus resulting in less biotinylation of PLP compared with WT M6a.

The critical role of EC2 of M6a described by the present study is in agreement with studies published on the functional importance of the EC2 of tetraspannins. It has been firmly established that the functional specificity of tetraspanins is determined by the EC2 region. For example, strong CD151 association with integrins requires the Gln^{194}–Arg^{195}–Asp^{196} site in the EC2 loop of CD151. Mutation of the QRD site not

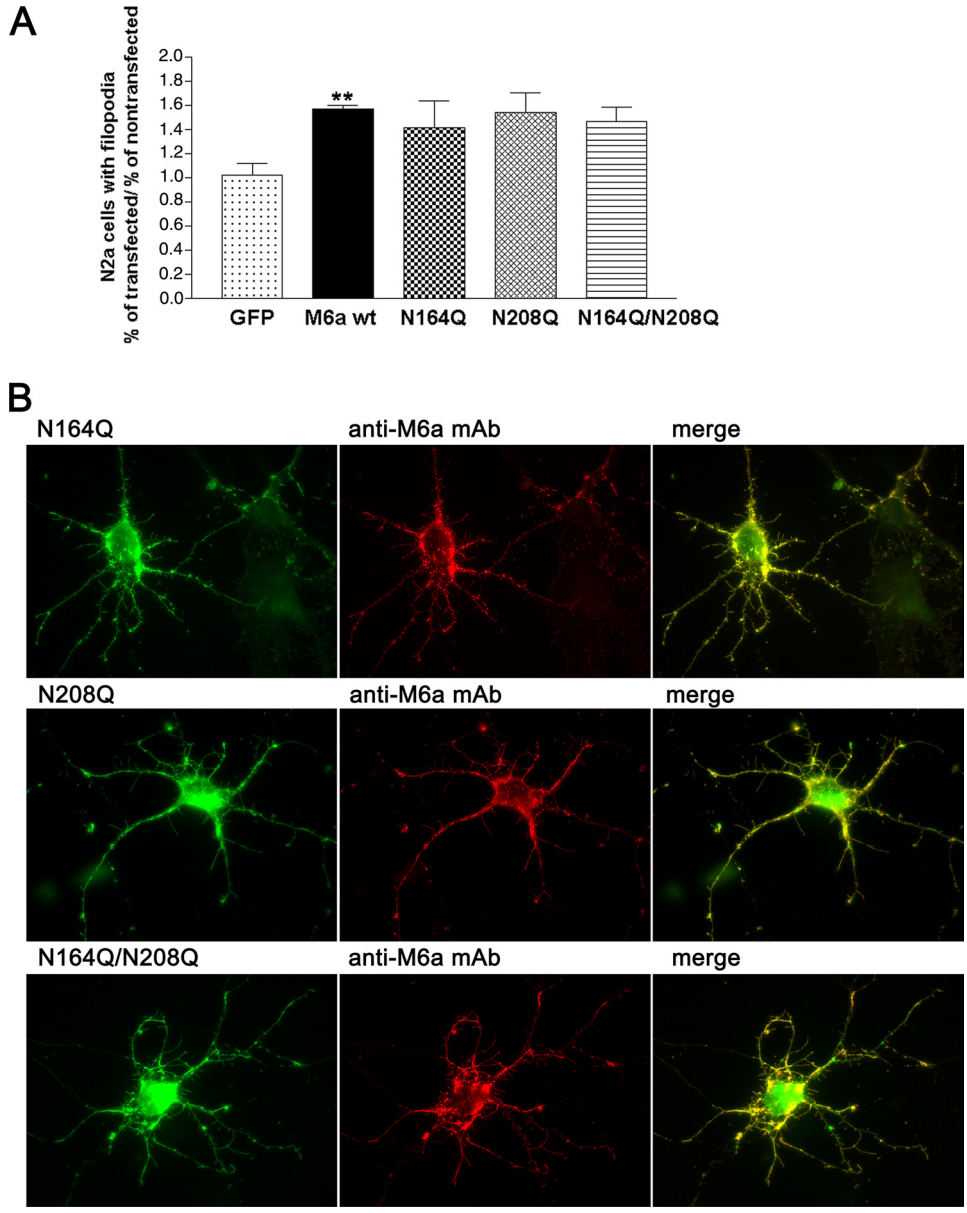

FIGURE 9. ***N*-Glycosylation mutants of M6a in the large extracellular domain (EC2).** *A*, effect of overexpression of N164Q, N208Q, and double N164Q/N208Q mutants of M6a on filopodium formation in the neuroblastoma cell line N2a. Cells were transfected, fixed, stained, and quantified as described under "Experimental Procedures." No differences have been observed for the effect of M6a mutants N164Q, N208Q, and double N164Q/N208Q on filopodia formation when compared with WT M6a. One-way ANOVA, p value 0.1375; **, p 0.0074 M6a WT *versus* GFP calculated with Student's t two tailed test. Data are means ± S.E. of ~59–121 cells per group from multiple experiments. *B*, mutations of Asn^{164} and Asn^{208} in the EC2 region do not prevent epitope recognition by mAb against M6a. Primary hippocampal neurons were transfected with the indicated GFP-tagged mutants and fixed as described under "Experimental Procedures." Immunostaining was done with rat anti-M6a mAb in non-permeabilized cells. Goat anti-rat IgG labeled with Alexa Fluor 546 was used as a secondary antibody. Images show complete colocalization in cells transfected with mutants N164Q, N208Q, and double N164Q/N208Q. *Bar* = 10 μm.

only causes loss of integrin association, but also disrupts integrin-dependent cell spreading (19). An additional example of the functional importance of EC2 in tetraspanins is the human brain-specific tetraspanin TM4SF2/A15 that is associated with mental retardation when inactivated by a point mutation, P172H. Notably, P172H also lies within the variable region of EC2 (30). This is also true in the case of peripherin/rds, a tetraspanin expressed exclusively in retinal rod and cone photoreceptor cells. Mutations of peripherin/rds lead to several retinal diseases in humans. The majority (about 70%) of the peripherin/rds mutations that cause disease are located within EC2 (31).

We speculate that EC2 of M6a may be involved in mediating specific lateral homotypic and/or heterotypic interactions with other partner molecules (transmembrane proteins or soluble ligands) that have to be identified and C174A and C192A mutations may lead to the loss of this intermolecular association. This hypothesis is based on the fact that the role of tetraspanins is mediated by their ability to interact with numerous proteins. Tetraspanins are involved in primary direct interactions with transmembrane proteins, including immunoglobulin superfamily members EWI-2 and EWI-F (32, 33), Claudin-1 (34), epidermal growth factor receptor membrane-bound ligands (35), integrins (36), other tetraspanins forming homodimers (37), as well as intracellular proteins such as syntenin-1 (38). In addition, secondary interactions of tetraspanins include not only multiple distinct tetraspanins, and many other transmembrane proteins (39), but also signaling enzymes such as PKC isoforms (40) and phosphatidylinositol 4-kinase (41). Through the network of homotypic and heterotypic interactions, tetraspanins regulate the spatial juxtaposition of associated proteins on the plasma membrane, which results in coordination of signaling pathways and cross-talk with cytoskeletal structures (11, 42, 43). The putative protein-protein interaction sites of M6a may map to EC2, and the alteration of EC2 conformation by Cys → Ala mutations would thus affect its function supposedly by changing its ability to interact with potential binding partners. The identification of the M6a interactions is thus the next important step that would provide further information about possible signaling pathways or protein-protein interactions through which M6a could act to affect neuronal remodeling.

Our hypothesis that the potential M6a interactions with external ligands and/or specific homo/heterotypic protein-protein interactions could consequently regulate signaling pathways inside the cell is well justified by the previous finding that monoclonal anti-M6a antibody directed against the extracellu-

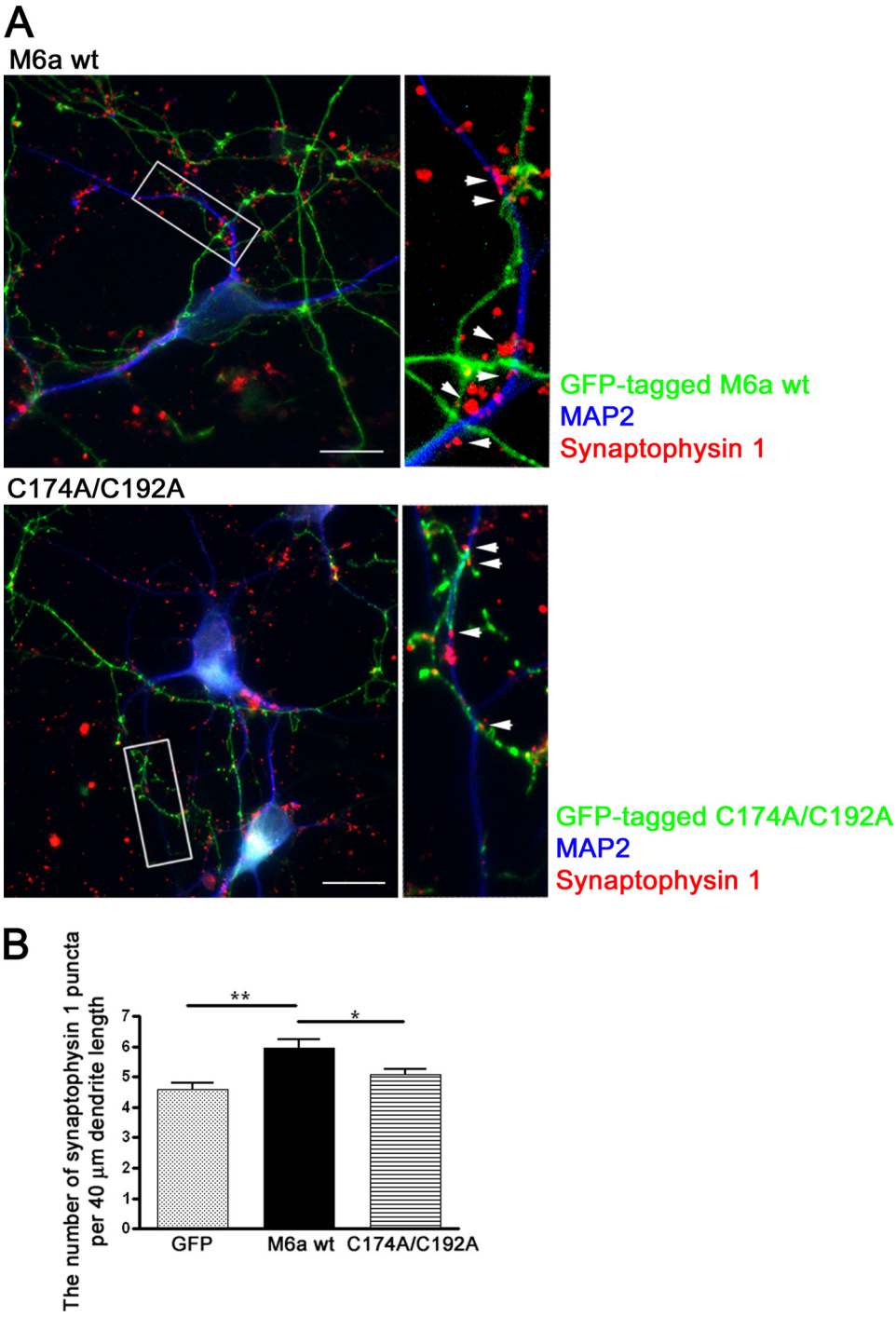

FIGURE 10. **EC2 cysteine mutant C174A/C192A affects synaptic density in primary hippocampal neurons.** *A*, neurons after 9 days *in vitro* were transfected with GFP-tagged C174A/C192A mutant, WT M6a, and GFP alone. Neurons were fixed as previously described and co-immunostained with the antibodies against synaptophysin 1 (*red*) to visualize synaptic puncta and MAP2 (*blue*), a specific marker for dendrites. To quantify the spots of synaptophysin 1 immunoreactivity (indicated by *arrows*), regions were selected where transfected axons (identified by green labeling and their lack of MAP2 immunostaining) contacted non-transfected MAP2 positive dendrites (*A*, *maximized views*). *Bar* = 20 μm. *B*, the graph shows that dendrites that are in contact with WT M6a expressing axons display significantly higher density of presynaptic clusters compared with the dendrites that are in contact with C174A/C192A transfected axons (one-way ANOVA, ***, *p* value 0.0004; Tukey's multiple comparison test, **, $p < 0.001$, GFP *versus* M6a WT; $p > 0.05$, GFP *versus* C174A/C192A; *, $p < 0.05$, M6a WT *versus* C174A/C192A). Data plotted represent means ± S.E.

We demonstrate that the same mutations (C174A and C192A) in EC2 that prevent epitope recognition by a function blocking anti-M6a mAb also affect filopodium formation and synaptic cluster density. Moreover, we show that the cysteines but not the asparagine residues within EC2 are critical for the optimal recognition and functioning of EC2. The replacement of the Asn^{164} and Asn^{208}, two conserved amino acid residues within EC2 different from cysteines, did not have any effect on cell membrane localization of the M6a protein, filopodium formation, and did not interfere with the binding of function blocking anti-M6a antibody. We also show that the lack of epitope recognition by the anti-M6a antibody is not due to the failure of the mutated protein to reach the cell surface. As shown by its accessibility to the digestion with extracellular PK, the C174A/C192A mutant is inserted into the plasma membrane and is exposed on the outside of the cell. These data are in agreement with the observations that specific mAbs against some tetraspanins, for example, the anti-CD151 mAbs, TS151r (21), and 8C3 (20), can disrupt the associations between partner proteins and tetraspanins (19–21). Mutating the TS151r binding site in CD151 led to functional changes in integrin-dependent spreading (19), and the removal of CD151 from $\alpha 3\beta 1$-integrin by the mAb 8C3 led to the reduced binding of the stripped integrin to laminin (20). Interestingly, the site of interaction between CD151 and the $\alpha 3$-integrin has been mapped to the QRD sequence in the CD151 EC2.

The small extracellular domain (EC1) is not a part of a surface-exposed epitope recognized by the antibody. The mutations of cysteine residues Cys^{44} and Cys^{46} in EC1 do not affect the cell membrane localization of the M6a protein and its recognition by a function blocking anti-M6a mAb. But although the mutations of Cys^{44} and Cys^{46} in EC1 do not interfere with the binding of anti-M6a antibody, they do slightly interfere with filopodium formation. We suggest that EC1 contributes to the optimal functioning of the protein lar part of the protein interferes with the extension of neurites by cultured cerebellar neurons (6). In the present study we provide evidence that EC2 is a functional surface-exposed epitope of M6a recognized by the function blocking anti-M6a antibody.

tein in the induction of filopodial protrusion formation. This would be in accordance with M6a structural analogy to tetraspanins. Although there is little known about the structure and function of EC1 in tetraspanins, in one study where EC1 from CD81 was replaced with a short linker sequence, EC1 was shown to be required for optimal expression of EC2, but not for binding to the hepatitis C virus E2 protein (44). Besides, it has been shown that in tetraspanins, monoclonal antibodies that recognize cell surface epitopes so far exclusively recognize EC2.

Another possibility is that Cys → Ala mutations within EC2 disrupt lateral interactions indirectly by affecting the proper packing of M6a TMDs. Tetraspanin TMDs have been shown to be involved in crucial intramolecular and intermolecular interactions that are essential for correct intramolecular folding and intermolecular associations with other transmembrane proteins in tetraspanin-enriched domains (45). Notably, a recent study by Wu *et al.* (46) that identified the μ-opioid receptor to be associated with M6a demonstrated that TMDs 3 and 4 are required for direct interaction of the μ-opioid receptor-M6a.

M6a belongs to the proteolipid protein (PLP/DM20) family of myelin proteins (1) that includes glia-specific PLP/DM20, and neuron-specific M6a and M6b detected in both neuronal and glial populations (5, 47). Two distinct integrin α subunits mediate the outgrowth of processes in nerve and glial cells. Process extension by glial cells is likely to involve the α_V integrin. In contrast, α1 integrin, a laminin receptor, is up-regulated by nerve growth factor and other differentiation stimuli and involved in neurite extension by nerve cells (48). PLP/DM20 has been shown to participate in integrin receptor signaling in oligodendrocytes (49). It interacted directly with the cytoplasmic domain of the α_v integrin and this complex appeared important for binding of fibronectin to oligodendrocytes. PLP antibody specific for the extracellular loop domain of PLP inhibited binding of fibronectin to oligodendrocytes (49). Given the high degree of homology between M6a and PLP, it is also possible that M6a is related to integrin signaling.

A possible role of M6a in the formation of synapses has been suggested (7, 10). In the mouse hippocampal tissue, M6a mRNA expresses in granule cells of the dentate gyrus and pyramidal neurons in CA1 and CA3. Immunoreactivity for M6a is concentrated in the regions of relatively dense synaptic contact (10). Accordingly, ultrastructural studies have located M6a immunoreactivity in the synapses of the rat cerebellum and in the axon terminals of the rat cerebellar molecular layer (50). Moreover, neuroanatomical data demonstrated that M6a is an axonal component of glutamatergic neurons and that it is localized to distinct sites of the axonal plasma membrane of pyramidal and granule cells in adult rat forebrain and cerebellum (51). In the mouse retina, the expression of M6a parallels that of the presynaptic protein, synaptophysin (7). In our previous study, we found reduced synaptophysin immunoreactivity and lower synaptic cluster density in cultures with decreased M6a levels (10). It has been established that synapse formation by dissociated neurons in culture strongly correlates with focal accumulations of structures that can be labeled with antibodies against synaptic vesicle proteins, such as synaptophysin 1 and synapsin 1 (23). Our present study shows that dendrites that are in contact with EC2 mutant C174A/C192A expressing axons display significantly lower density of presynaptic clusters compared with the dendrites that are in contact with WT M6a-transfected axons.

It has been observed that profound changes in the morphology of the mossy fiber terminals and significant loss of synapses are detected in hippocampal formation of chronically stressed and corticosterone-treated rats. These alterations are partially reversible following rehabilitation from stress or corticosterone treatments (29). Thus, with respect to the apparent enrichment of M6a within mossy fibers (51) and the fact that in hippocampal formation chronic stress reduces M6a mRNA expression (2, 3), it appears feasible that M6a may regulate presynaptic plasticity possibly by mediating molecular interactions with specific partner molecules and the EC2 domain with its four cysteine residues playing a crucial role. Consequently, stress-induced changes in M6a expression may modify the molecular interactions with functional consequences for neuronal remodeling.

REFERENCES

1. Yan, Y., Lagenaur, C., and Narayanan, V. (1993) *Neuron* **11,** 423–431
2. Alfonso, J., Frick, L. R., Silberman, D. M., Palumbo, M. L., Genaro, A. M., and Frasch, A. C. (2006) *Biol. Psychiatry* **59,** 244–251
3. Alfonso, J., Pollevick, G. D., Van Der Hart, M. G., Flügge, G., Fuchs, E., and Frasch, A. C. (2004) *Eur. J. Neurosci.* **19,** 659–666
4. Boks, M. P., Hoogendoorn, M., Jungerius, B. J., Bakker, S. C., Sommer, I. E., Sinke, R. J., Ophoff, R. A., and Kahn, R. S. (2008) *Am. J. Med. Genet. Part B Neuropsychiatric Genet.* **147,** 707–711
5. Yan, Y., Narayanan, V., and Lagenaur, C. (1996) *J. Comp. Neurol.* **370,** 465–478
6. Lagenaur, C., Kunemund, V., Fischer, G., Fushiki, S., and Schachner, M. (1992) *J. Neurobiol.* **23,** 71–88
7. Zhao, J., Iida, A., Ouchi, Y., Satoh, S., and Watanabe, S. (2008) *Mol. Vis.* **14,** 1623–1630
8. Mukobata, S., Hibino, T., Sugiyama, A., Urano, Y., Inatomi, A., Kanai, Y., Endo, H., and Tashiro, F. (2002) *Biochem. Biophys. Res. Commun.* **297,** 722–728
9. Michibata, H., Okuno, T., Konishi, N., Wakimoto, K., Kyono, K., Aoki, K., Kondo, Y., Takata, K., Kitamura, Y., and Taniguchi, T. (2008) *Stem Cells Dev.* **17,** 641–651
10. Alfonso, J., Fernández, M. E., Cooper, B., Flugge, G., and Frasch, A. C. (2005) *Proc. Natl. Acad. Sci. U.S.A.* **102,** 17196–17201
11. Hemler, M. E. (2005) *Nat. Rev. Mol. Cell Biol.* **6,** 801–811
12. Kitadokoro, K., Bordo, D., Galli, G., Petracca, R., Falugi, F., Abrignani, S., Grandi, G., and Bolognesi, M. (2001) *EMBO J.* **20,** 12–18
13. Seigneuret, M., Delaguillaumie, A., Lagaudrière-Gesbert, C., and Conjeaud, H. (2001) *J. Biol. Chem.* **276,** 40055–40064
14. Stipp, C. S., Kolesnikova, T. V., and Hemler, M. E. (2003) *Trends Biochem. Sci.* **28,** 106–112
15. Davidson, F. F., Loewen, P. C., and Khorana, H. G. (1994) *Proc. Natl. Acad. Sci. U.S.A.* **91,** 4029–4033
16. Brocco, M., Pollevick, G. D., and Frasch, A. C. (2003) *J. Neurosci. Res.* **74,** 744–753
17. Weimbs, T., and Stoffel, W. (1992) *Biochemistry* **31,** 12289–12296
18. Higginbottom, A., Quinn, E. R., Kuo, C. C., Flint, M., Wilson, L. H., Bianchi, E., Nicosia, A., Monk, P. N., McKeating, J. A., and Levy, S. (2000) *J. Virol.* **74,** 3642–3649
19. Kazarov, A. R., Yang, X., Stipp, C. S., Sehgal, B., and Hemler, M. E. (2002) *J. Cell Biol.* **158,** 1299–1309
20. Nishiuchi, R., Sanzen, N., Nada, S., Sumida, Y., Wada, Y., Okada, M., Takagi, J., Hasegawa, H., and Sekiguchi, K. (2005) *Proc. Natl. Acad. Sci. U.S.A.* **102,** 1939–1944
21. Serru, V., Le Naour, F., Billard, M., Azorsa, D. O., Lanza, F., Boucheix, C., and Rubinstein, E. (1999) *Biochem. J.* **340,** 103–111
22. Cohen-Cory, S. (2002) *Science* **298,** 770–776
23. Fletcher, T. L., Cameron, P., De Camilli, P., and Banker, G. (1991) *J. Neu-*

rosci. **11,** 1617–1626
24. Donohue, H. S., Gabbott, P. L., Davies, H. A., Rodríguez, J. J., Cordero, M. I., Sandi, C., Medvedev, N. I., Popov, V. I., Colyer, F. M., Peddie, C. J., and Stewart, M. G. (2006) *Neuroscience* **140,** 597–606
25. Magariños, A. M., and McEwen, B. S. (1995) *Neuroscience* **69,** 89–98
26. Magariños, A. M., and McEwen, B. S. (1995) *Neuroscience* **69,** 83–88
27. Magariños, A. M., Verdugo, J. M., and McEwen, B. S. (1997) *Proc. Natl. Acad. Sci. U.S.A.* **94,** 14002–14008
28. Sandi, C., Davies, H. A., Cordero, M. I., Rodriguez, J. J., Popov, V. I., and Stewart, M. G. (2003) *Eur. J. Neurosci.* **17,** 2447–2456
29. Sousa, N., Lukoyanov, N. V., Madeira, M. D., Almeida, O. F., and Paula-Barbosa, M. M. (2000) *Neuroscience* **97,** 253–266
30. Zemni, R., Bienvenu, T., Vinet, M. C., Sefiani, A., Carrié, A., Billuart, P., McDonell, N., Couvert, P., Francis, F., Chafey, P., Fauchereau, F., Friocourt, G., des Portes, V., Cardona, A., Frints, S., Meindl, A., Brandau, O., Ronce, N., Moraine, C., van Bokhoven, H., Ropers, H. H., Sudbrak, R., Kahn, A., Fryns, J. P., Beldjord, C., and Chelly, J. (2000) *Nat. Genet.* **24,** 167–170
31. Kohl, S., Giddings, I., Besch, D., Apfelstedt-Sylla, E., Zrenner, E., and Wissinger, B. (1998) *Acta Anat.* **162,** 75–84
32. Stipp, C. S., Kolesnikova, T. V., and Hemler, M. E. (2001) *J. Biol. Chem.* **276,** 40545–40554
33. Stipp, C. S., Orlicky, D., and Hemler, M. E. (2001) *J. Biol. Chem.* **276,** 4853–4862
34. Kovalenko, O. V., Yang, X. H., and Hemler, M. E. (2007) *Mol. Cell. Proteomics* **6,** 1855–1867
35. Iwamoto, R., Higashiyama, S., Mitamura, T., Taniguchi, N., Klagsbrun, M., and Mekada, E. (1994) *EMBO J.* **13,** 2322–2330
36. Berditchevski, F. (2001) *J. Cell Sci.* **114,** 4143–4151
37. Kovalenko, O. V., Yang, X., Kolesnikova, T. V., and Hemler, M. E. (2004) *Biochem. J.* **377,** 407–417
38. Latysheva, N., Muratov, G., Rajesh, S., Padgett, M., Hotchin, N. A., Overduin, M., and Berditchevski, F. (2006) *Mol. Cell Biol.* **26,** 7707–7718
39. Tarrant, J. M., Robb, L., van Spriel, A. B., and Wright, M. D. (2003) *Trends Immunol.* **24,** 610–617
40. Zhang, X. A., Bontrager, A. L., and Hemler, M. E. (2001) *J. Biol. Chem.* **276,** 25005–25013
41. Yauch, R. L., and Hemler, M. E. (2000) *Biochem. J.* **351,** 629–637
42. Levy, S., and Shoham, T. (2005) *Physiology* **20,** 218–224
43. Levy, S., and Shoham, T. (2005) *Nat. Rev. Immunol.* **5,** 136–148
44. Masciopinto, F., Campagnoli, S., Abrignani, S., Uematsu, Y., and Pileri, P. (2001) *Virus Res.* **80,** 1–10
45. Kovalenko, O. V., Metcalf, D. G., DeGrado, W. F., and Hemler, M. E. (2005) *BMC Struct. Biol.* **5,** 11
46. Wu, D. F., Koch, T., Liang, Y. J., Stumm, R., Schulz, S., Schröder, H., and Höllt, V. (2007) *J. Biol. Chem.* **282,** 22239–22247
47. Werner, H., Dimou, L., Klugmann, M., Pfeiffer, S., and Nave, K. A. (2001) *Mol. Cell Neurosci.* **18,** 593–605
48. Tarone, G., Hirsch, E., Brancaccio, M., De Acetis, M., Barberis, L., Balzac, F., Retta, S. F., Botta, C., Altruda, F., Silengo, L., and Retta, F. (2000) *Int. J. Dev. Biol.* **44,** 725–731
49. Gudz, T. I., Schneider, T. E., Haas, T. A., and Macklin, W. B. (2002) *J. Neurosci.* **22,** 7398–7407
50. Roussel, G., Trifilieff, E., Lagenaur, C., and Nussbaum, J. L. (1998) *J. Neurocytol.* **27,** 695–703
51. Cooper, B., Werner, H. B., and Flügge, G. (2008) *Brain Res.* **1197,** 1–12